Numerical simulation of accidental released hazardous gas dispersion at a methanation plant using GASFLOW-MPI

Han Zhang [a], *Simon Sauerschell* [b], *Qingxin Ba* [c,d], *Guang Hu* [d], *Thomas Jordan* [d], *Siegfried Bajohr* [b], *Jianjun Xiao* [d,*]

[a] *Institute of Nuclear and New Energy Technology, Collaborative Innovation Center of Advanced Nuclear Energy Technology, Key Laboratory of Advanced Reactor Engineering and Safety of Ministry of Education, Tsinghua University, Beijing 100084, China*
[b] *Engler Bunte Institute, Fuel Technology, EBI ceb, Karlsruhe Institute of Technology, Karlsruhe, 76131, Germany*
[c] *Institute of Thermal Science and Technology, Shandong University, Jinan 250061, China*
[d] *Institute for Thermal Energy Technology and Safety (ITES), Karlsruhe Institute of Technology, Karlsruhe, 76021, Germany*

HIGHLIGHTS

- The safety evaluation of accidental release in the methanation plant is performed.
- Both toxicity and flammability of the hazardous gas cloud are analyzed.
- A local global two step strategy is used to predict the hazardous gas dispersion.
- Performances of two different types of exhaust pipes are compared and discussed.

Keywords:
Turbulence dispersion
Hydrogen safety
Hazardous gas
Power to Gas technology

ABSTRACT

Power to Gas technologies could play an important role in future energy systems, since they make it possible to store surplus electric energy from fluctuating renewable energy sources such as solar and wind. In Power to Gas concepts, the first step towards storage is the production of H_2 by electrolysis, a possible further step is methanation. The Engler Bunte Institute, Fuel Technology at Karlsruhe Institute of Technology is conducting research on catalytic methanation in slurry bubble column reactors, which represent a highly load flexible reactor technology. To obtain experimental data at a semi industrial scale a methanation pilot plant was built and commissioned. The plant is equipped with various safety valves, which may release the hazardous gases H_2, CO and CH_4 in the chemical reactor into the environment in the unintended case of overpressure, which may lead to a flammable and/or toxic cloud, threatening the safety of the workers and other humans near the plant. In this work, the safety evaluation of the accidental release in the methanation plant is performed using the numerical tool GASFLOW MPI. Both toxicity and flammability of the hazardous gas cloud are analyzed and discussed. A local global two step simulation strategy, including a local computational model and a global computational model, is employed to calculate the hazardous gas dispersion efficiently and accurately. In the first step, a local detailed computational model with fine mesh is used to calculate the release mass flow through the exhaust tube and the complicated shock waves

* *Corresponding author.*
E mail address: jianjun.xiao@kit.edu (J. Xiao).

directly without any further assumption model such as the notional nozzle model. In the second step, a large scale model with the relatively coarse mesh is chosen to efficiently predict the hazardous gas dispersion around the entire methanation plant. Moreover, the performances of two different types of exhaust pipes are compared and discussed, and the recommended exhaust pipe design is provided. The simulation results show that version B of the exhaust tubes is more recommendable from the viewpoint of safety.

Introduction

With a rapidly increasing of renewable energy, storing surplus electric energy becomes a critical issue, due to the fluctuating availability of renewable energy sources such as solar and wind. Power to Gas technology is a promising solution for surplus electric energy management because of its high storage capacity potential [1,2]. In the Power to Gas technol ogy, hydrogen is produced by electrolysis firstly and then it is used to produce hydrocarbon fuels, such as the methane, which can be fed into the existing natural gas grid or can be liquefied and long term stored as liquid natural gas (LNG). Specifically, methane could be generated in an industrial scale methanation plant by the methanation reaction using CO_2 or CO as the carbon source brought to resection with H_2 [1]. Within the research project Energy Lab 2.0 at Karlsruhe Institute of Technology, a suitable methanation pilot plant was built. Process design and commissioning was conducted by Engler Bunte Institute, Fuel Technology. Plant construc tion was carried out by FRINTEC GmbH Frankfurt, Germany. The plant is equipped with various safety valves, which may release the gases CO, H_2 and CH_4 into the environment in the unintended case of overpressure thus creating a flammable and toxic cloud in the surroundings of the plant.

Obviously, a successful prediction of the hazardous gas cloud distribution is the first but critical step for an accurate safety analysis of the methanation plant. Compared with the traditional integral model [3,4], the Computational Fluid Dy namics (CFD) method could provide more accurate simulation results and resolves more detailed fluid dynamic information, especially for the engineering application with complex geometrical configuration. With the development of the computational capability, various CFD codes have been well developed and widely used in the prediction of the heat and mass transfer phenomenon in the large scale industrial fa cility, such as FLACS [5], ADREA HF [3,6], TONUS [7], PHOEN ICS [8], CFD ACE [9], CFX [10], Fluent [11,12], Code Saturne [13,14] and OpenFoam [15]. S. Manogaran [11] and H. Wilken ing [9] use the CFD codes Fluent and CFD ACE to simulate the hydrogen and methane dispersion process in the pipeline system. E. Kashi [10] analyzes the gas dispersion of an offshore platform with a comprehensive CAD geometrical model using the commercial CFD code CFX. P. Middha [5] utilizes the CFD code FLACS to predict a range of hydrogen turbulence mixing and dispersion process in the benchmarks and engineering applications, such as the low momentum releases and sub sonic jets in a garage, as well as the turbulence jet released from high pressure vessels. However, in most existing research, the release mass flow is simplified as a constant chock flow or modeled by the notional nozzle model near the nozzle region due to the lack of shock wave capture capability [5,10]. All these approximation models are based on the assumption that the stagnation pressure in the reservoir is a constant, while, in most practical engineering applications, all the stagnation parameters are always time varied. To the authors' best knowledge, there are no published studies on the unintended release process with the varied stagnation parameters using the same solver within one CFD software framework. The challenging issue is that, during this release process, it includes the complicated shock wave structure near the nozzle and the incompressible dispersion process in the far away region. The Mach number covers a wide range from incompressible flow to compressible flow and the all speed flow capability is required. Additionally, compared with the safety assessment regarding the garage [3,16], tunnel [17,18], and pipeline system [9,11], the literature is scarce to address gas dispersion after the accidental release of haz ardous gases from safety valves.

Therefore, the hazardous gas dispersion released from the exhaust pipes in the three phase methanation plant is con ducted in this work using the CFD code GASFLOW MPI. GAS FLOW MPI is a well validated all speed CFD code, which could successfully simulate a wide region of Mach number flow

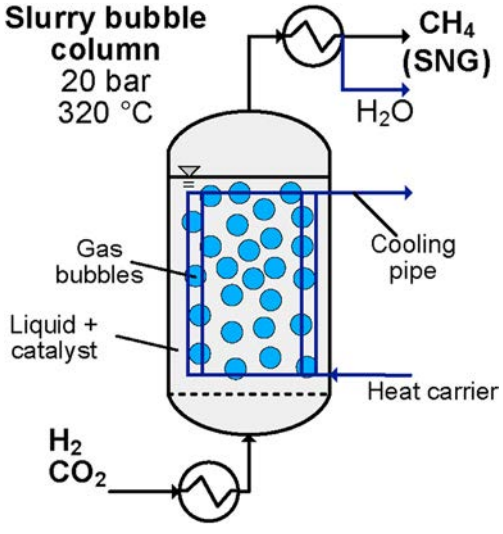

Fig. 1 – Three-phase-reactor (slurry bubble column) of the methanation plant (modified after Lefebvre, J., 2015 [30]).

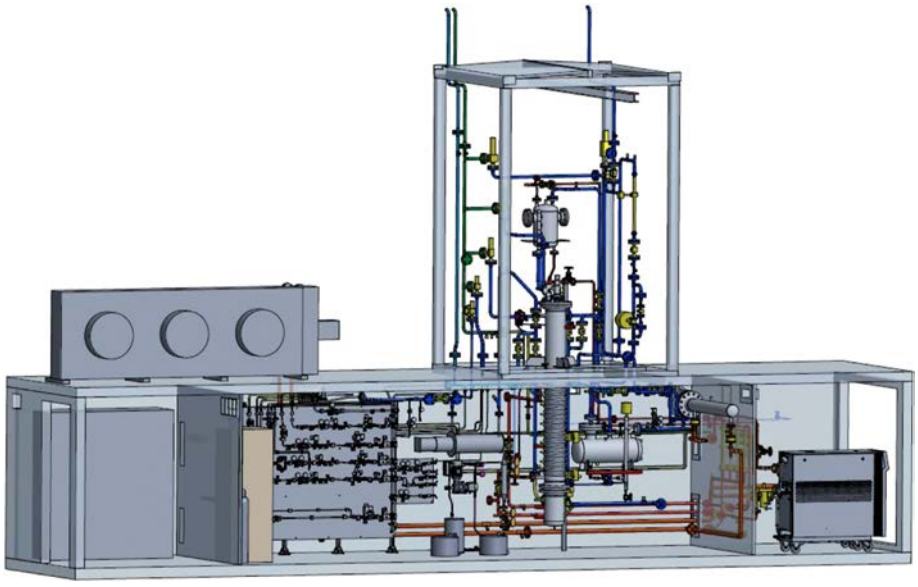

Fig. 2 – 3D-drawing of the three-phase methanation plant (by FRINTEC GmbH Frankfurt, Germany).

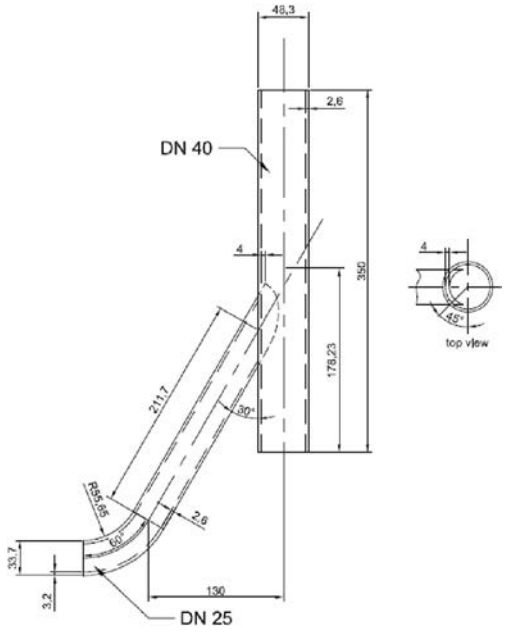

Fig. 3 – Exhaust tube (Version A).

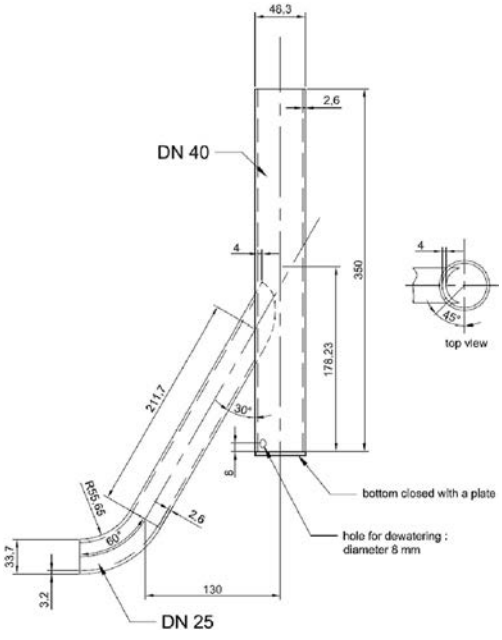

Fig. 4 – Exhaust tube (Version B).

using one solver, from the incompressible flow to compress ible flow, even the supersonic flow with the complicated shock wave [19]. All the key phenomenon in this work have been validated in the previous work, including the compli cated shock wave structures [19,20], the turbulent jet flow [19,21] as well as the dispersion process in the large scale in dustry facilities [22,23]. The simulation results of GASFLOW MPI have well accepted for the accidental released hazard ous gas dispersion analysis [24–29]. The main contributions of this work are that:

(1) Due to the all speed capability of GASFLOW MPI, the transient process in the reservoir and the release mass flow could be calculated directly without any further assumption model like the notional nozzle model.
(2) The hazardous gas cloud distribution released from the exhaust pipes of the methanation plant is analyzed and its safety risk is evaluated. The performances of two different types of exhaust pipes are compared and dis cussed, and the recommended exhaust pipe design is provided.

This paper is arranged as follows: The background of the methanation plant and its exhaust tube configurations, as well as the accident scenarios are described in section

Table 1 – Scenarios considered in dispersion calculation.

	Scenario	Hazard	Opening pressure (bar)	Closing pressure (bar)	Fluid temperature
Case 1	Syngas (H_2, CO, CO_2, N_2)	CO poisoning/Explosive atmosphere	25	20	Ambient temperature 20 °C
Case 2	CH_4	Explosive atmosphere	25	20	Ambient temperature 20 °C

Methanation plant and its exhaust tubes; Section Simulation model provides the simulation model of the methanation plant, including the computational domain information, the mesh distributions and the basic physical model; The simulation results of the hazardous gas disperse with two different exhaust pipe configurations are presented in section Simulation results and discussion; and The main conclusions are presented in section Conclusion.

Methanation plant and its exhaust tubes

Methanation plant

The heart of the methanation plant is the three phase reactor, as shown in Fig. 1, where a solid catalyst is suspended in a liquid heat carrier (dibenzyl toluene) in the slurry bubble column and is fluidized by the gaseous educts (H_2 and CO_2 and/or CO). The gases are dissolved in the liquid phase and react on the surface of the catalyst particles, as shown in Eqs. (1) and (2). The products, CH_4 and H_2O, are transferred back into the gaseous phase and leave the reactor at the top. Because of the exothermic reaction cooling must be provided to maintain the reactor temperature of 300 °C. The pressure inside the reactor is 20 bar. After leaving the reactor, the products are cooled to ambient temperature to condense water.

CO Methanation

$$CO\,(g) + 3H_2\,(g) \rightarrow CH_4\,(g) + H_2O\,(g)\ \Delta_R H^0 \quad 206\ \text{kJ/mol} \quad (1)$$

CO_2 Methanation

$$CO_2\,(g) + 4H_2\,(g) \rightarrow CH_4\,(g) + 2H_2O\,(g)\ \Delta_R H^0 \quad 165\ \text{kJ/mol} \quad (2)$$

The 3D drawing of the methanation plant is shown in Fig. 2 which is a pilot plant built in a modified 40 foot shipping container with the support from the project Energy Lab 2.0 at Karlsruhe Institute of Technology. A tower is mounted on top of the shipping container to allow the installation of the bubble column reactor which has an overall height of 3 m. Three exhaust tubes are installed at the top of the container tower. The second tube from the left is connected to the safety valves, whereas the other ones are for minor gas flows such as exhaust gases from gas sampling. The reactor and other apparatus inside the plant are protected to avoid the over pressure states by safety valves that open at around 25 bar and close again at 20 bar. When the safety valves are open, the gases in the reactor go through the safety valves and are released into the atmosphere directly from the exhaust tubes.

Exhaust tube design

Two different types of exhaust tubes were designed for this three phase methanation plant following the indications given by DVGW guideline G 442 (M) [31]. According to the guideline, the bottom of the exhaust tube should be completely open in order to prevent rainwater from entering the plant, (see Fig. 3, named as "Version A" in the following). However, for high flow rate situations, the exhaust gases may leave the tube not only from the top but also from the bottom, which may lead to explosive or toxic atmospheres at ground level. In that case, the guideline allows closing up the bottom of the tube and leave just a small opening for dewatering (see Fig. 4, named as "Version B" in the following). The detailed geometric information about these two types of exhaust tubes are provided in Figs. 3 and 4, respectively.

Accidental release scenarios

When the pressure in the reactor is higher than the normal designed value due to unwanted events, the safety valves will open and release the gases from the reactor into the atmosphere through the exhaust tubes. It may form a flammable and/or toxic cloud at ground level and may threaten the safety of the workers and other persons near the plant. The release process will stop when the reactor pressure is lower than valves closing pressure and the safety valves close

Table 2 – Summarized information about simulated cases.

	Accident scenarios	
	Syngas	CH_4
Model I	Exhaust tube (Version A)	Exhaust tube (Version A)
	Exhaust tube (Version B)	Exhaust tube (Version B)
Model II	Exhaust tube (Version A)	Exhaust tube (Version A)
	Exhaust tube (Version B)	Exhaust tube (Version B)

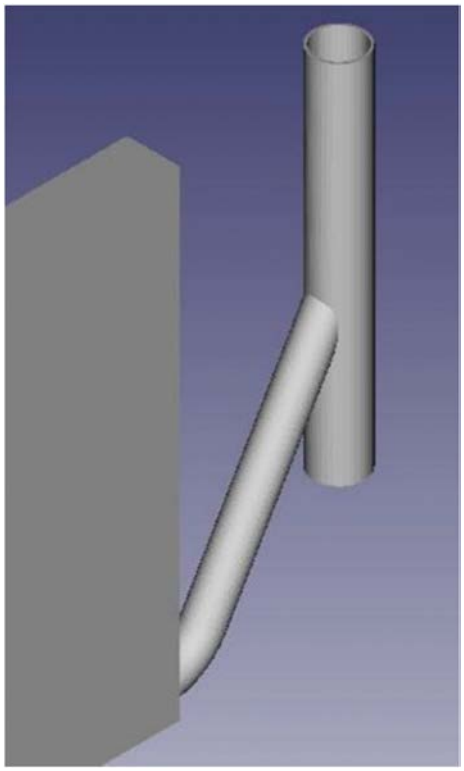

Fig. 5 – Local detailed model (Model I).

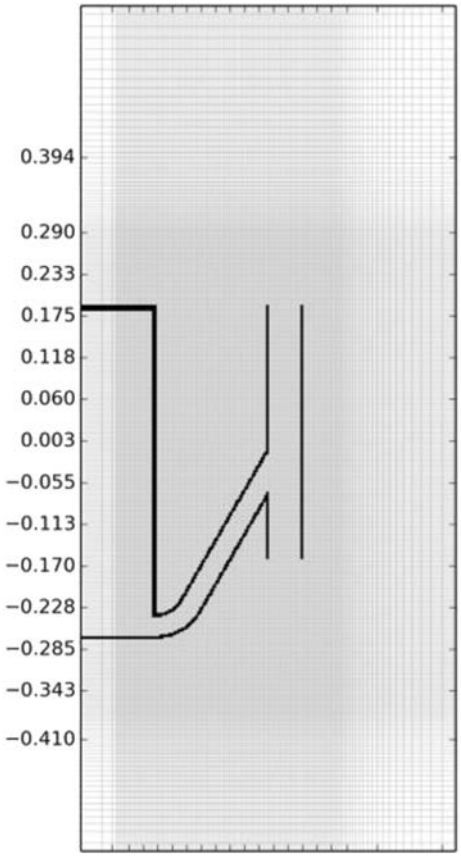

Fig. 6 – Computational model for exhaust tube (Version A).

again. The most unfavorable assumptions are considered in the accidental release scenarios to ensure results are conservative, as following:

- The higher concentrations of flammable or toxic gases, more total amount of released gases and higher gas velocities lead to the worse situation. Therefore, we assume that the safety valve has the highest opening pressure (25 bar absolute) and the lowest closing pressure (20 bar absolute).
- In the present case, the exhaust gases cause a more serious hazard when sinking to the ground instead of rising upwards. Therefore, the lowest expected gas temperatures and preferably gases with high densities are considered.
- Regarding the hazard of poisoning, the focus is set on carbon monoxide because of its high toxicity.

The components of the released gas are a mixture of reactants and reaction products at a certain mixing ratio. In this work, two typical accidental scenarios were identified, as listed in Table 1. In the first typical scenario, the released gas is the pure gas phase reactants without any reaction products, which is the mixture of CO, CO_2, N_2 and H_2. Its detailed components are 57% H_2, 19% CO, 12% CO_2, 12% N_2. Both flammability and toxicity of the released gas should be considered in this case. The second scenario is the pure reaction product CH_4. We focus on the flammability analysis in the second case.

Simulation model

In this section, the physical model and numerical method are presented and discussed in subsection Physical models and CFD code GASFLOW MPI. According to the accidental scenario, the release starts at the pressure of 25 bar in the reactor and ends at the pressure of 20 bar, therefore, the release mass flow and the release time highly depend on the time varied parameters in the three phase reactor of the methanation plant. A local global two step simulation strategy, including a local computational model and a global computational model, were used in this work to simulate this complicated accidental release efficiently and accurately. In the first step, a local detailed computational model (Model I) with fine mesh was used to calculate the release mass flow through the exhaust tube and tank pressure in the reactor directly without any further assumption model, which is presented in subsection Computational model for release mass flow calculation. The release mass flow and release time determined in this model were used as the input for the second model. In the second step, a large scale model with the relatively coarse mesh (Model II) was chosen to efficiently predict the hazardous gas dispersion in the surroundings of the methanation plant, which is introduced in subsection Computational model for environmental safety evaluation. Please note that for each model, two types of exhaust tubes and two typical accidental scenarios were considered, respectively. All these simulated cases are summarized in Table 2.

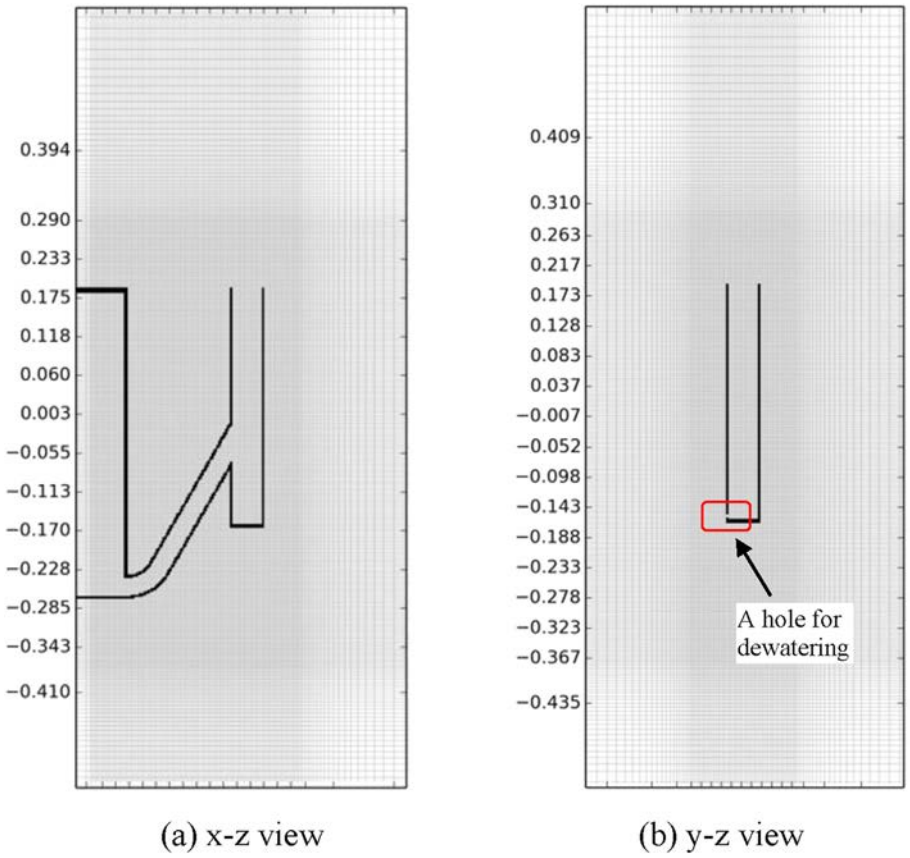

Fig. 7 – Computational model for exhaust tube (Version B).

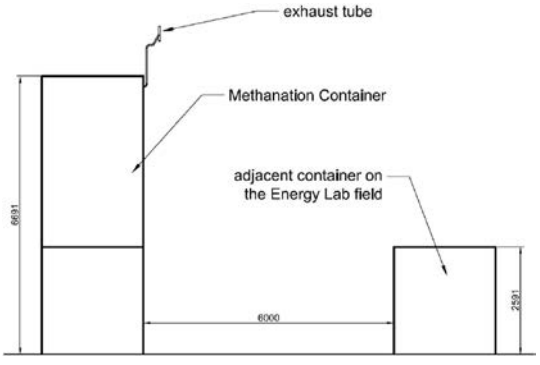

Fig. 8 – Methanation plant in y-z view.

Physical models and CFD code GASFLOW-MPI

GASFLOW MPI is a scalable parallel code specially designed for hazardous gases safety analysis. It has been validated by a serial of well known international blind/open benchmarks [19–23] and has been widely used to predict the hazardous gas cloud distribution and combustion dynamics behavior in the large scale industrial facilities during the past decades [24–27]. The three dimensional multi component compressible Navier–Stokes equations are solved by the powerful "all speed" ICE'd ALE algorithm. Due to its "all speed" capability, GASFLOW MPI could simulate the incompressible limited flow, compressible flow, and even the supersonic flow with the complicated shock wave in the same solver [19].

The turbulence model is a key issue for a successful simulation for the transport process of hazardous gases in the environment. The Detached Eddy Simulation (DES) model, a kind of LES/RANS hybrid turbulence model [21], is used in this work to model the turbulence effect, as shown in Eq. (3) Eq. (6). It could switch between LES model and RANS model adaptively according to the resolution of the turbulence, and has successfully applied in many engi neering problems [21,22]. The more detailed information about the DES model could be found in Ref. [21].

$$\frac{\partial}{\partial t}(\rho k) + \nabla \cdot (\rho k \mathbf{u}) \quad \nabla \cdot \left[\left(\mu + \frac{\mu_t}{\sigma_k}\right)\nabla k\right] + G_k + G_b \quad \frac{\rho k^{3/2}}{l_{des}} \tag{3}$$

$$\frac{\partial}{\partial t}(\rho \varepsilon) + \nabla \cdot (\rho \varepsilon \mathbf{u}) \quad \nabla \cdot \left[\left(\mu + \frac{\mu_t}{\sigma_\varepsilon}\right)\nabla \varepsilon\right] + C_1 \frac{\varepsilon}{k}(G_k + G_b) \quad C_2 \rho \frac{\varepsilon^2}{k} \tag{4}$$

$$l_{des} \quad \min(l_{k\varepsilon}, l_{les})\, l_{k\varepsilon} \quad \frac{k^{3/2}}{\varepsilon}\, l_{les} \quad C_{des}\Delta_{\max}\, \Delta_{\max} \quad \max(\Delta x, \Delta y, \Delta z) \tag{5}$$

$$\mu_t \quad \rho C_\mu \frac{k^2}{\varepsilon} \tag{6}$$

The second order accuracy Van Leer scheme is used for convection terms to capture the complicated shock wave structure in the exhaust tube and the second order accuracy

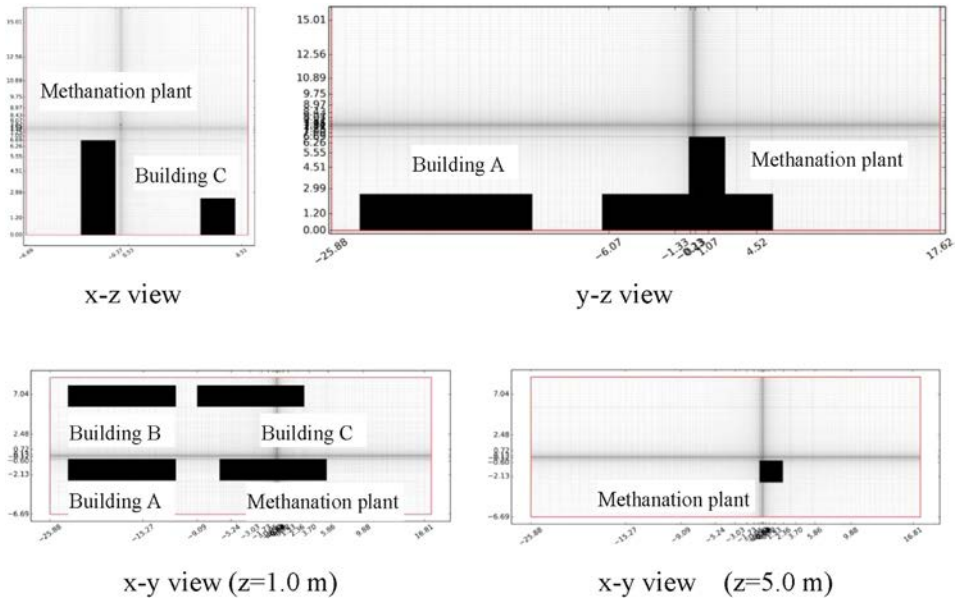

Fig. 9 – Computational domain and computational mesh for Model II.

center difference scheme is employed for the diffusion terms. The time step is determined adaptively based on the CFL number whose value is set to 0.5 in this work.

Computational model for release mass flow calculation

In this model (Model I), the computational domain includes the three phase reactor of the methanation plant and the entire exhaust tube with detailed geometry to directly calculate the release mass flow and tank pressure, as shown in Fig. 5. The tank volume is 200 L filled with high pressure reaction gases (see in Table 1). The initial gas pressure and temperature inside the reactor are 25 bar and 20 °C, respectively, and the safety valve is in the open state. The outside environmental temperature is set to 20 °C and the pressure is 1 bar. The detailed geometry information of the exhaust tube is shown in Figs. 3 and 4.

In order to resolve the detailed flow behavior in the exhaust tube, the mesh size is refined near the entire

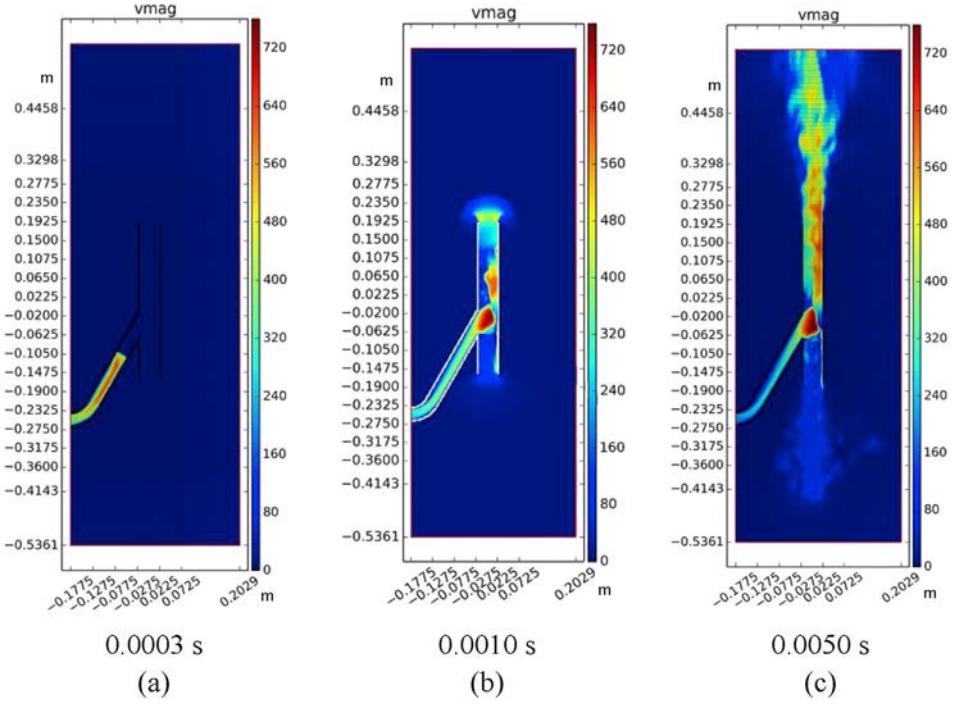

Fig. 10 – Velocity distribution of version A exhaust tube (x-z view).

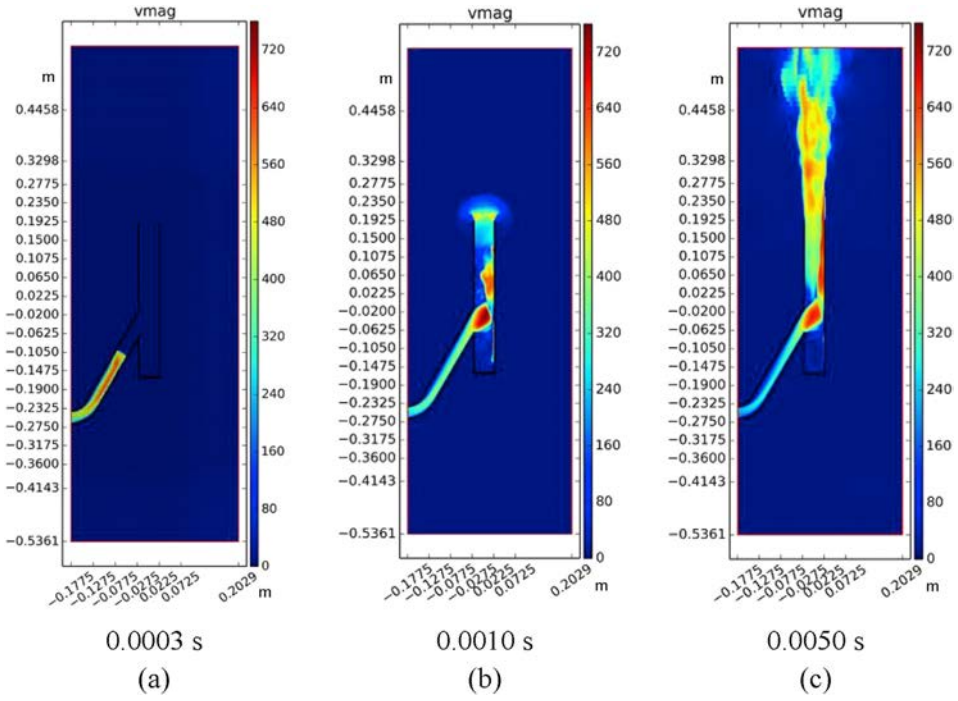

Fig. 11 – Velocity distribution of version B exhaust tube (x-z view).

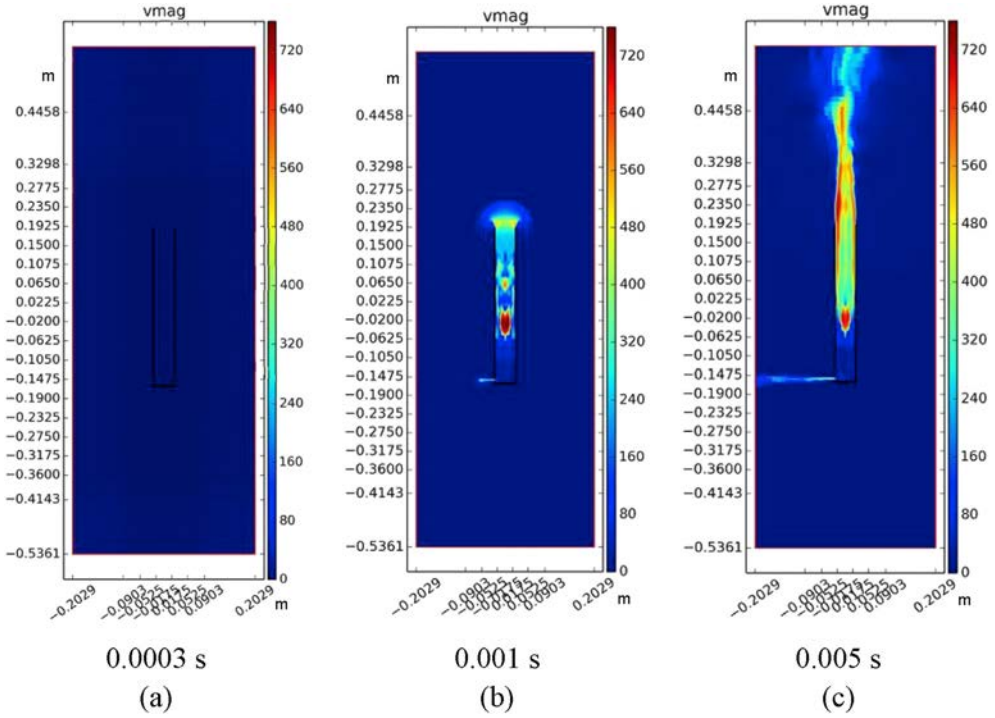

Fig. 12 – Velocity distribution of version B exhaust tube (y-z view).

exhaust tube with the minimum mesh size 0.058D, 0.058D, and 0.058D in x, y, z direction, respectively, where D 4.3 cm is the inner diameter of the exhaust tube. The gradually coarsened mesh is used for the region far away from the tube to save the computational cost. The total number of the computational mesh in this model is 5.94 million. Please note that the same mesh is used for both the exhaust tube of version A and version B. For the exhaust tube of version A, both the top and the bottom of tube are open, as shown in Fig. 6. While for the exhaust tube of

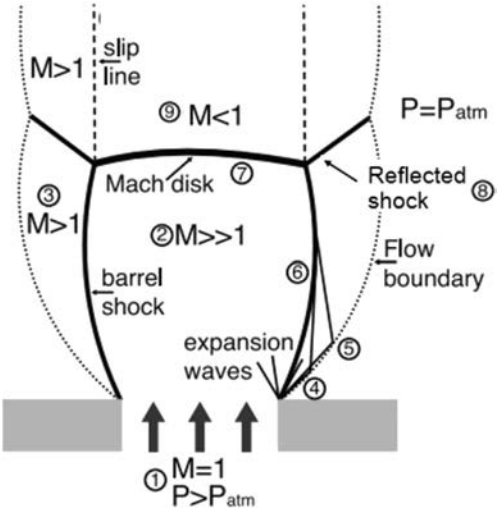

Fig. 13 e **Flow structure of an under-expanded jet [19].**

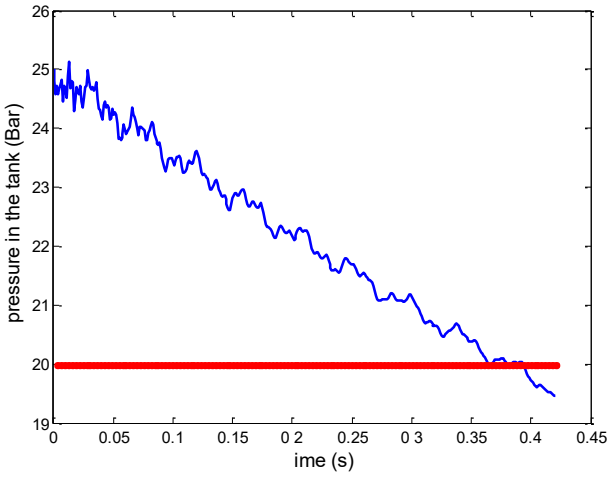

Fig. 16 e **Tank pressure in the three-phase-reactor.**

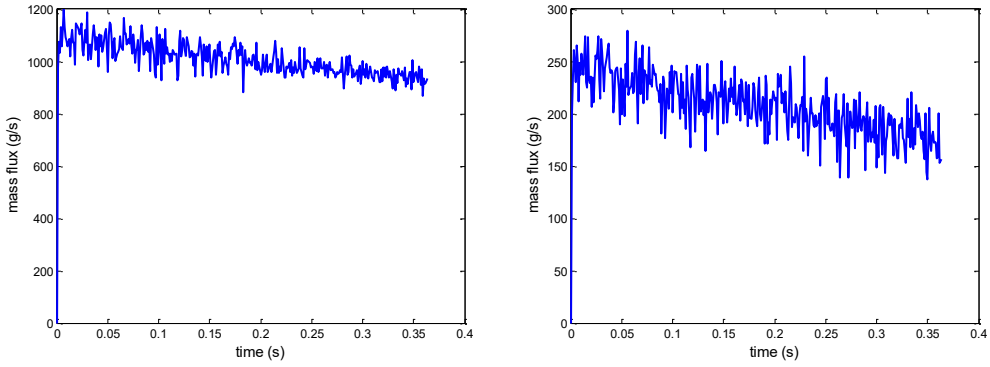

(a) mass flow at the top (b) mass flow at the bottom

Fig. 14 e **Mass flow rate of version A exhaust tube.**

version B, the bottom of tube is closed but with a small hole for dewatering, as shown in Fig. 7. For the shock wave case, the shock wave may reflect at the boundary condition if the boundary condition is not well defined. An additional buffer zone is used at the outside of the interested computational domain to avoid the shock wave reflection, where the large mesh size is used in the buffer region to dissipate the shock waves. The continuous boundary condition is posed at the outer surface of the buffer zone as the boundary condition.

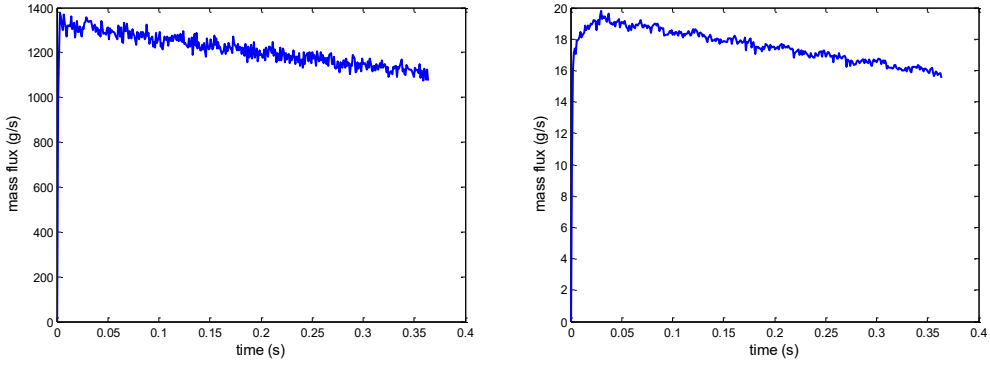

(a) mass flow at the top (b) mass flow at the bottom

Fig. 15 e **Mass flow rate of version B exhaust tube.**

Computational model for environmental safety evaluation

The second computational model (Model II) consists of the methanation plant and three other surrounding buildings to predict the hazardous gas cloud distribution and evaluate its safety risk, as shown in Fig. 8 and Fig. 9. The methanation plant is simplified as a combination of two rectangular solid structures with 12.19 m, 2.44 m and 6.69 m in x , y , z direc tion, respectively. The three surrounding buildings are also simply modeled as rectangular solid structures, as shown in Fig. 9. The size of building A and B is 12.30 m, 2.44 m and 2.6 m in x , y , z direction, respectively. Building C has the same size as building A and B in y , z direction, while its size in the x direction is 12.19 m. The entire computational domain used for this simulation is 43.50 m, 15.65 m, and 15.00 m in x , y , z direction, respectively.

The initial condition is set to the ambient temperature (20 °C) and ambient pressure (1 bar). The rigid no slip boundary condition with wall function model is used for the ground and continuous boundary condition is posed at the other boundaries. The time varied mass flow rate calculated in the Model I is used as the inlet boundary. The locations of the top and bottom release point are at (0, 0, 7.886 m) and (0, 0, 7.536 m), respectively. The relatively coarse mesh is used in this model to save computational time. The refined mesh is used near the release points to resolve the complicated transport phenomena near the nozzle. The minimum mesh size in x, y, z direction is set to 1.67 cm, 1.67 cm, and 2.5 cm, respectively, as shown in Fig. 9, and the mesh is gradually coarsened in the far field region. The total number of computational cells is 671,055.

Simulation results and discussion

In this section, the simulation results of two accidental sce narios are presented. For each accidental scenario, the local model (Model I) for release mass flow calculation and global

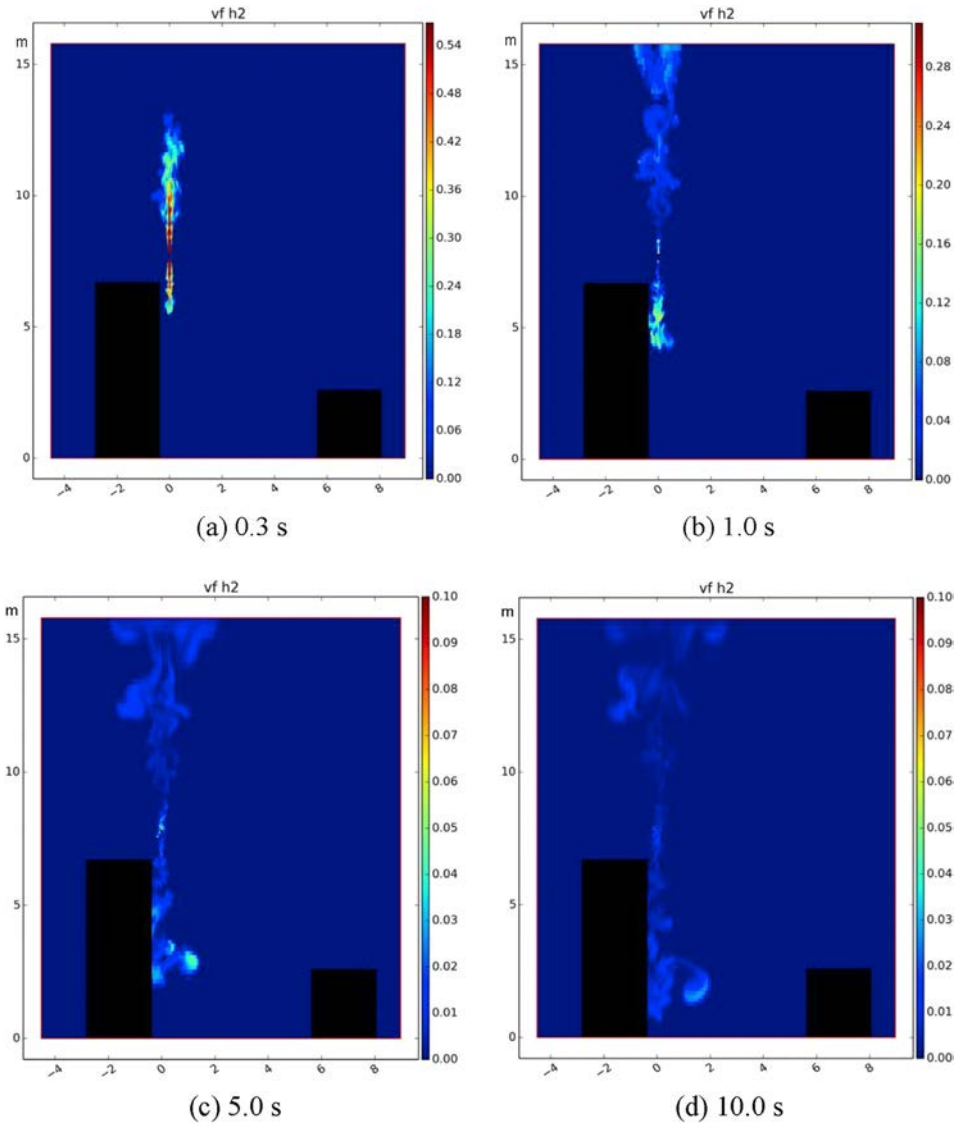

Fig. 17 – Hydrogen volume fraction distribution of version A exhaust tube (x-z view).

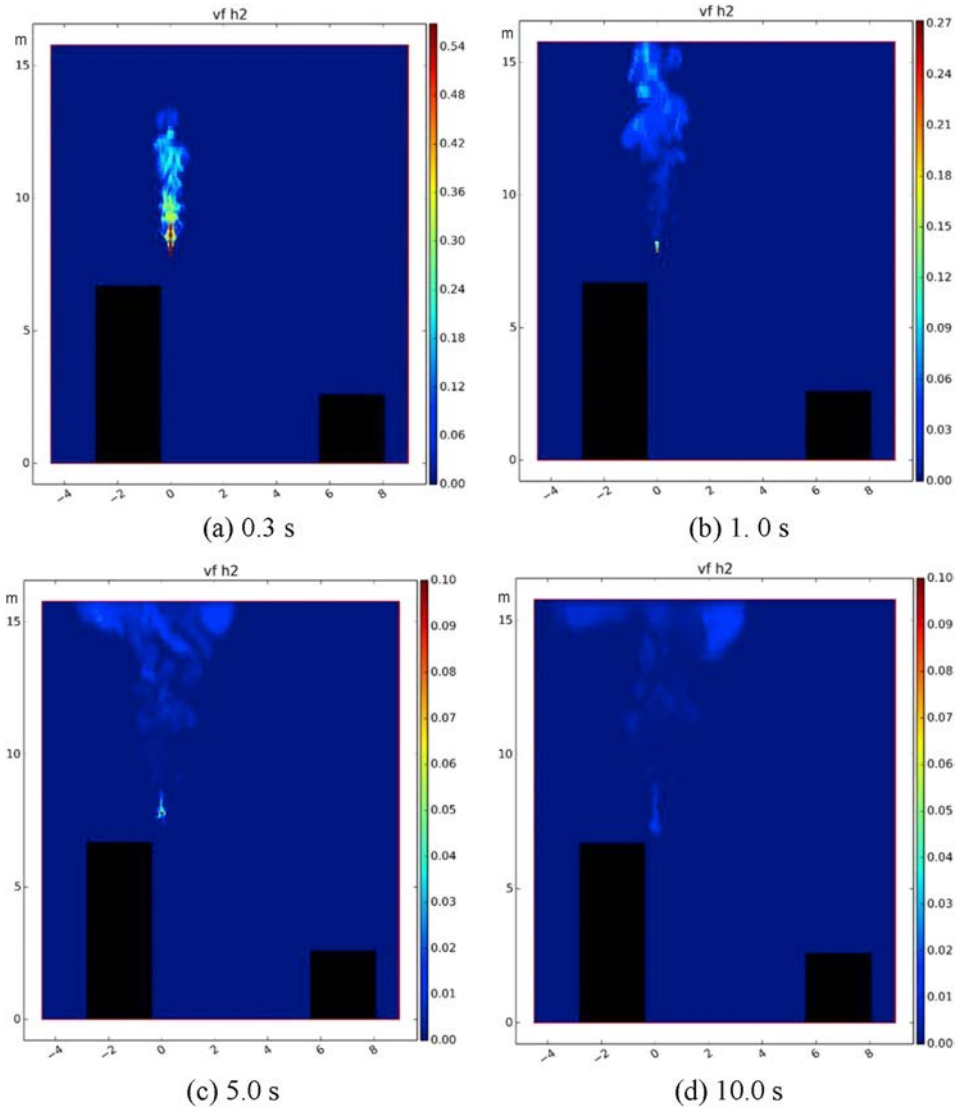

Fig. 18 – Hydrogen volume fraction distribution of version B exhaust tube (x-z view).

model (Model II) for environmental safety evaluation are dis cussed, respectively, and the performances of different exhaust tubes are also compared. The release of the syngasis predicted in subsection Syngas release case, where both toxicity and flammability of the hazardous gas cloud are evaluated and discussed. In subsection Methane release case, the methane dispersion results and its flammability are analyzed.

Syngas release case

Results of local model for release mass flow calculation

For the Model I (local model), the detailed release processes of syngas with different exhaust tubes are analyzed, as shown in Fig. 10, Fig. 11 and Fig. 12. In detail, Fig. 10 presents the velocity distribution of the version A exhaust tube. While Figs. 11 and 12 show the results of the version B exhaust tube in the x z view and y z view, respectively. Since the safety valve is set to be open as the initial condition, the mixed gas begins to release and flow into the exhaust tube. The velocity profile at 0.0003s shows that there is a velocity front in the tube formed by the high speed released mixed gas and the still air, and the central velocity of the mixed gas is higher than that near the pipe wall due to the wall friction, as shown in Figs. 10(a) and Fig. 11(a) (The terms "vmag" in Figs. 10 and 11 are short for velocity magnitude.). Then, the high pressured mixed gas enters the vertical pipe section, accelerates due to the expansion at the intersection of two pipe sections, and finally impinges on the wall of the vertical pipe section, as shown in Figs. 10(b), 11(b) and 12(b). It also shows that there is a shock wave when the mixed gas goes into the atmosphere.

In detail, when the high pressured gas is released in the open large space, the typical flow pattern could be divided into several regions, as shown in Fig. 13. The high pressured gas would undergo a Prandtl Meyer expansion when it en ters into the intersection of the pipe sections, as shown in Figs. 10 (b) and Fig. 11 (b). Due to this Prandtl Meyer expansion effect, the flow is rapidly accelerated and

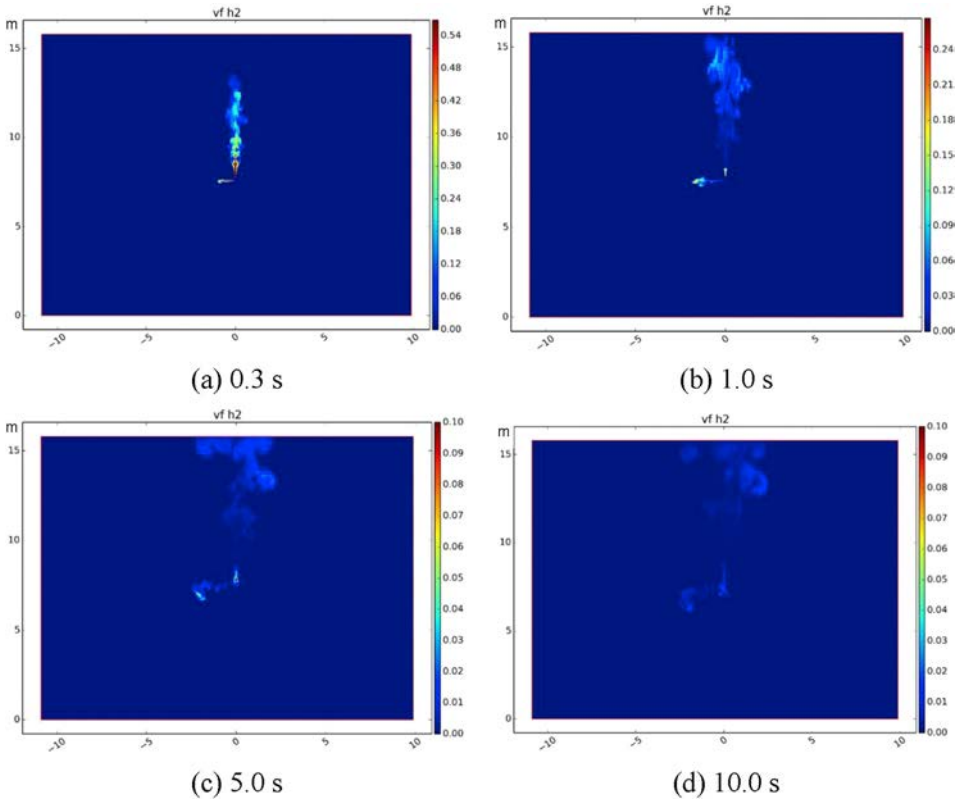

Fig. 19 – Hydrogen volume fraction distribution of version B exhaust tube (y-z view).

reaches the peak of velocity, as shown in Figs. 10 (b) and Fig. 11 (b). A continuous series of expansion waves are formed at the nozzle orifice (seen in Fig. 13) and then the pressure of the ambient gas at the boundary pushes the over expanded fluid back, generating the barrel shock, as shown in Figs. 10 (b), Fig. 11 (b) and Fig. 13. In this release case, the turbulent jet impinges on the side of the tube finally (seen in Figs. 10 (b) and Fig. 11 (b)).

The performances of different types of exhaust tubes are significantly different when the released gas moves outside the exhaust tubes. For version A exhaust tube, as shown in Fig. 10(c), the mixed gas is released from both top and the bottom ports, respectively, forming two ver tical free jets. The mass flow through the top port is about 4 times higher than that through the bottom port since that the angle of inclination at the junction of the two pipes is not vertical, as shown in Figs. 10(c) and Fig. 14. Moreover, with the increase of the gas release, the critical mass flow gradually decreases (see Fig. 14) due to the reduced pressure in the three phase reactor. While for version B exhaust tube, most of the mixed gas is released from both top port, since the bottom port is closed and only a small hole is remained, as shown in Figs. 11(c), Fig. 12(c). The released gas from the bottom hole forms a horizontal jet flow, which is different from the vertical jet of version A exhaust tube. The mass flux released from the bottom hole is approximately one seventieth of that from the top port (see Fig. 15).

During the release period, the tank pressure gradually de creases from 25 bar, and finally reaches the closing pressure of the safety valve (20 bar) when the release time gets to 0.39 s (see Fig. 16). Therefore, for the syngas release scenarios, the release time is 0.39 s, and then the safety valve is closed. The time varied mass flows from the top and the bottom ports during the release phase could be determined by this local model (Model I), as shown in Figs. 14 and 15. The release time and the time varied mass flows are used as the input for the global model (Model II) for safety evaluation.

Results of global model for environmental safety evaluation

By using Model II (global model), the hazardous gas dispersion at the pilot scale methanation plant with its surrounding buildings is simulated. For the syngas release case, both the flammability and the toxicity of the hazardous gas cloud are evaluated.

Since hydrogen is more flammable than carbon monox ide (CO) and the volume of hydrogen (57%) in the released gas is significantly larger than that of carbon monoxide (19%), hydrogen is chosen to perform the flammability risk evaluation. It is well known that the explosive range of hydrogen in air is 4.0%–75.6%. The hydrogen distributions of the different exhaust tubes are shown in Fig. 17, Fig. 18 and Fig. 19, and (The terms "vf" in Figs. 17–19 are short for volume fraction H_2.). For version A exhaust tube, two vertical jets are released from the top port and bottom port respectively during the period between 0 s and 0.39 s. The upward jet is released at a height of about 8 m, and then mixed with the surrounding air, as shown in Fig. 17. The downward jet flows along the outside of the methanation container, as shown in Fig. 17 (a), and moves further toward

the ground due to the inertia even though the release phase is finished, as shown in Fig. 17(b–d). The maximum hydrogen volume fraction at ground level is lower than 3% (below the lower explosive limit of hydrogen) when it rea ches 10 s, as shown in Fig. 17 (d). For version B exhaust tube, there is an upward vertical jet and a horizontal jet, as shown in Figs. 18 and 19. Compared with the case of version A exhaust tube, almost all of the released hydrogen is located at a height above 5 m, which is relatively far from ground level and thus from the persons working there or

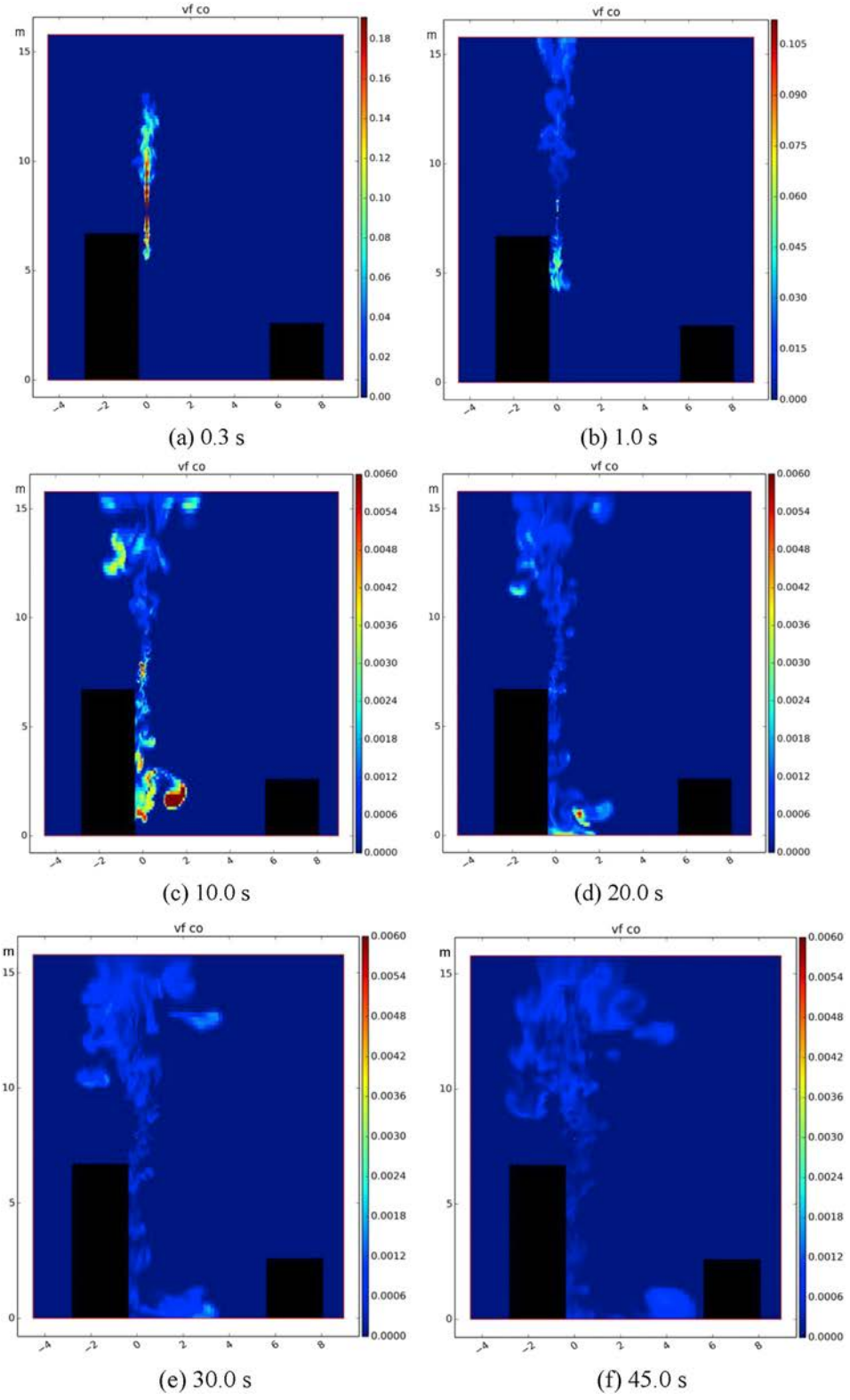

Fig. 20 – CO volume fraction distribution of version A exhaust tube (x-z view).

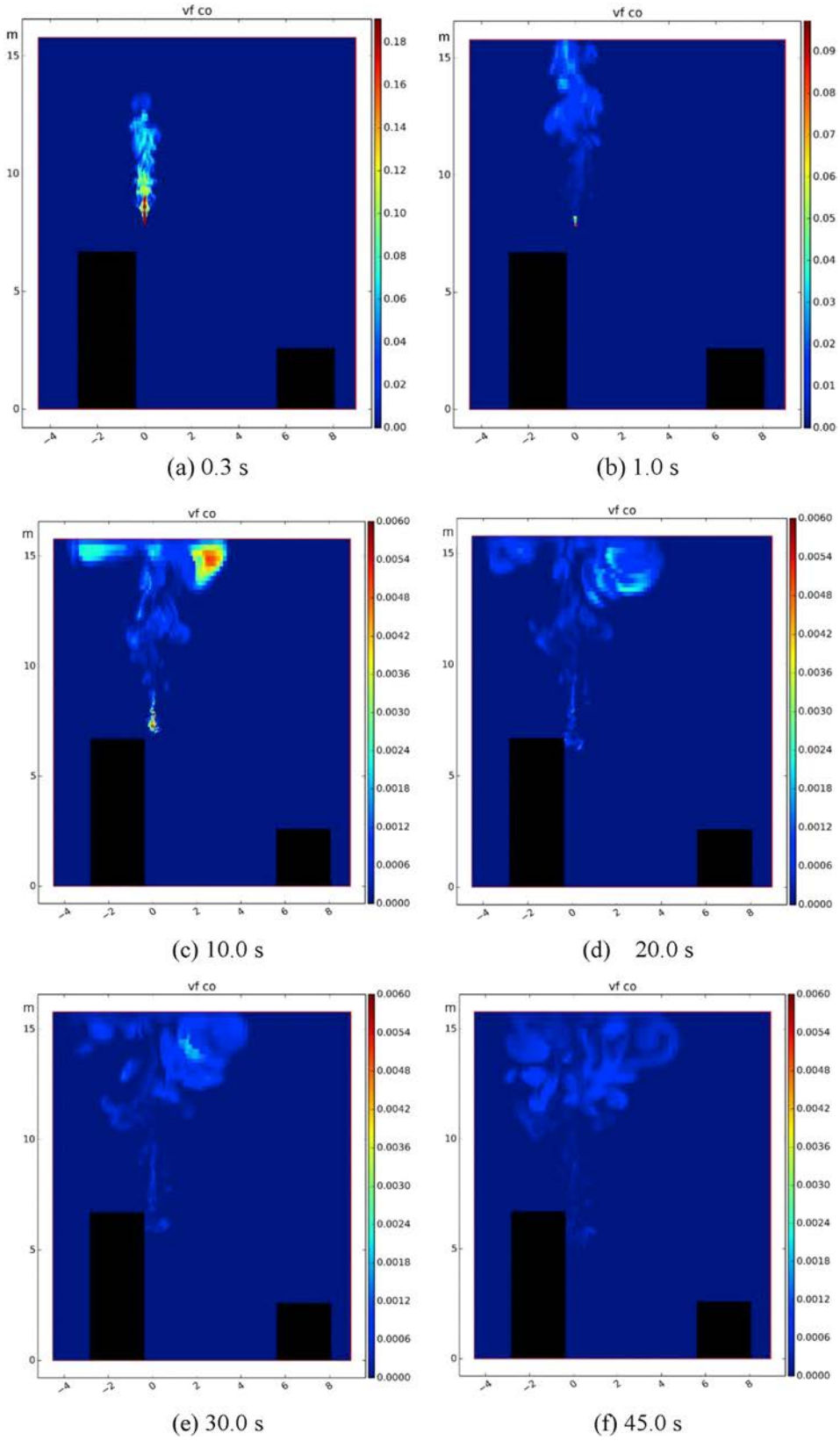

Fig. 21 – CO volume fraction distribution of version B exhaust tube (x-z view).

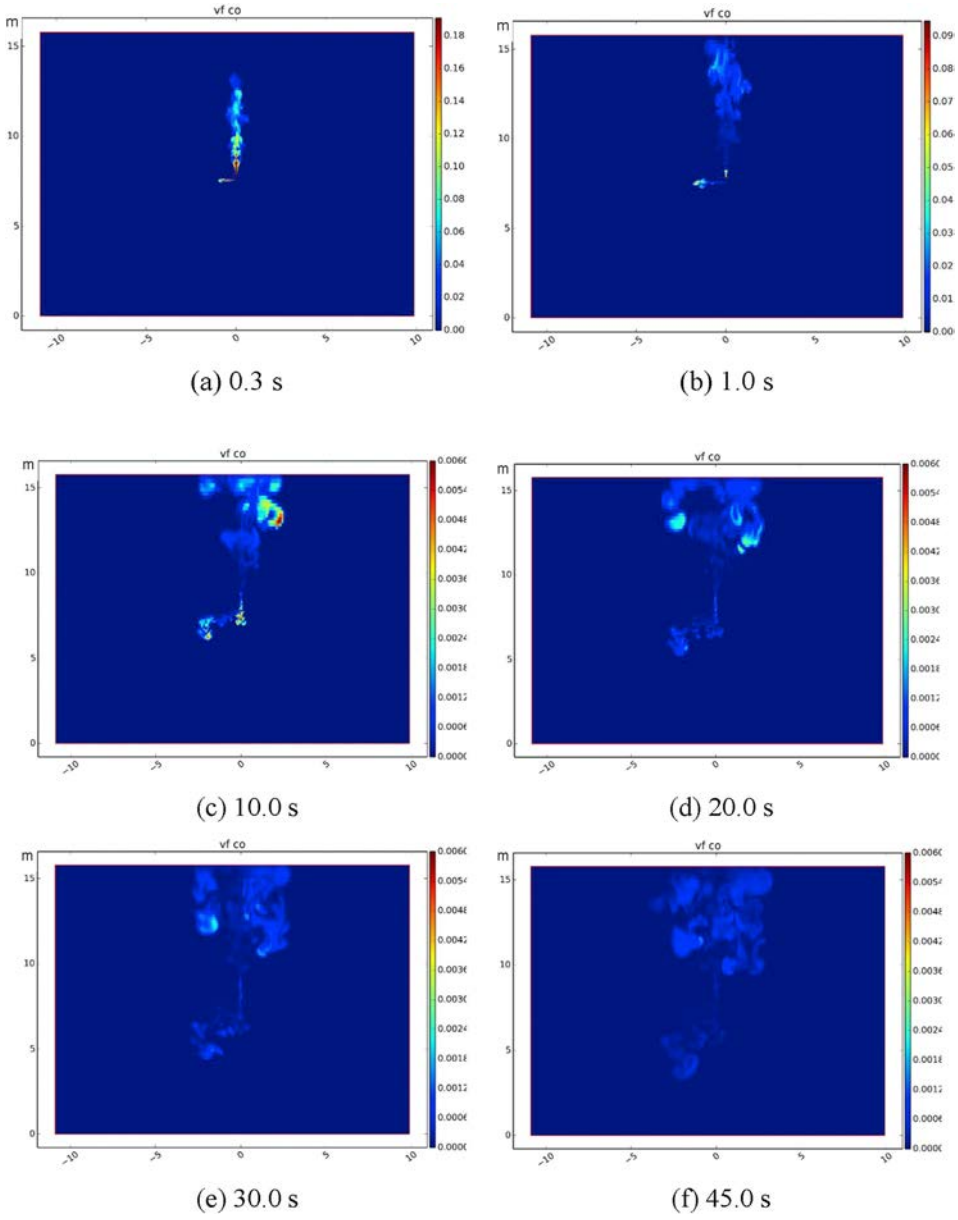

Fig. 22 – CO volume fraction distribution of version B exhaust tube (y-z view).

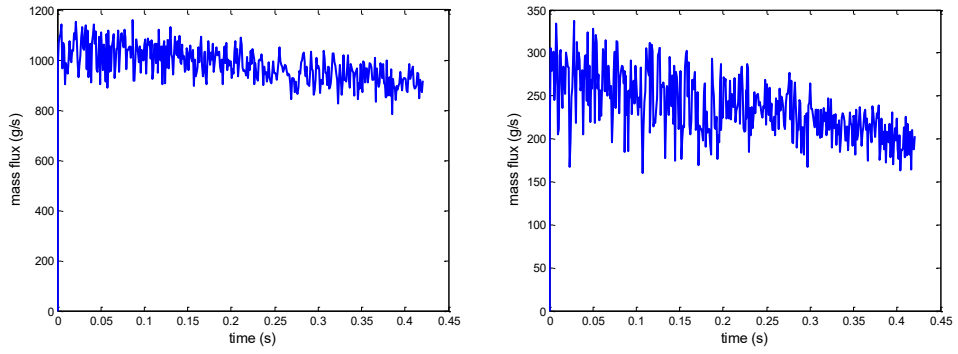

(a) mass flow at the top (b) mass flow at the bottom

Fig. 23 – Mass flow rate of Version A exhaust tube (Methane).

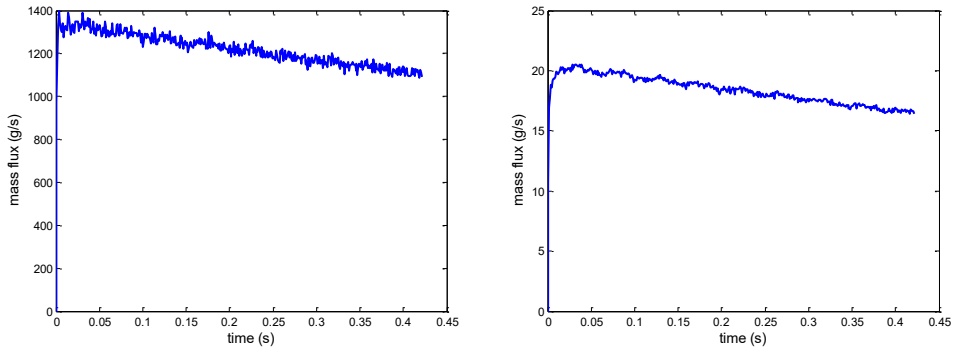

(a) mass flow at the top (b) mass flow at the bottom

Fig. 24 e Mass flow rate of Version B exhaust tube (Methane).

passing through. Moreover, the maximum hydrogen vol ume fraction is about 2% at 10 s, which is also lower than that of the version A exhaust tube.

An evaluation of the effect on the surroundings caused by the highly toxic carbon monoxide is also performed. According to the Acute Exposure Guideline Levels 3 (AEGL

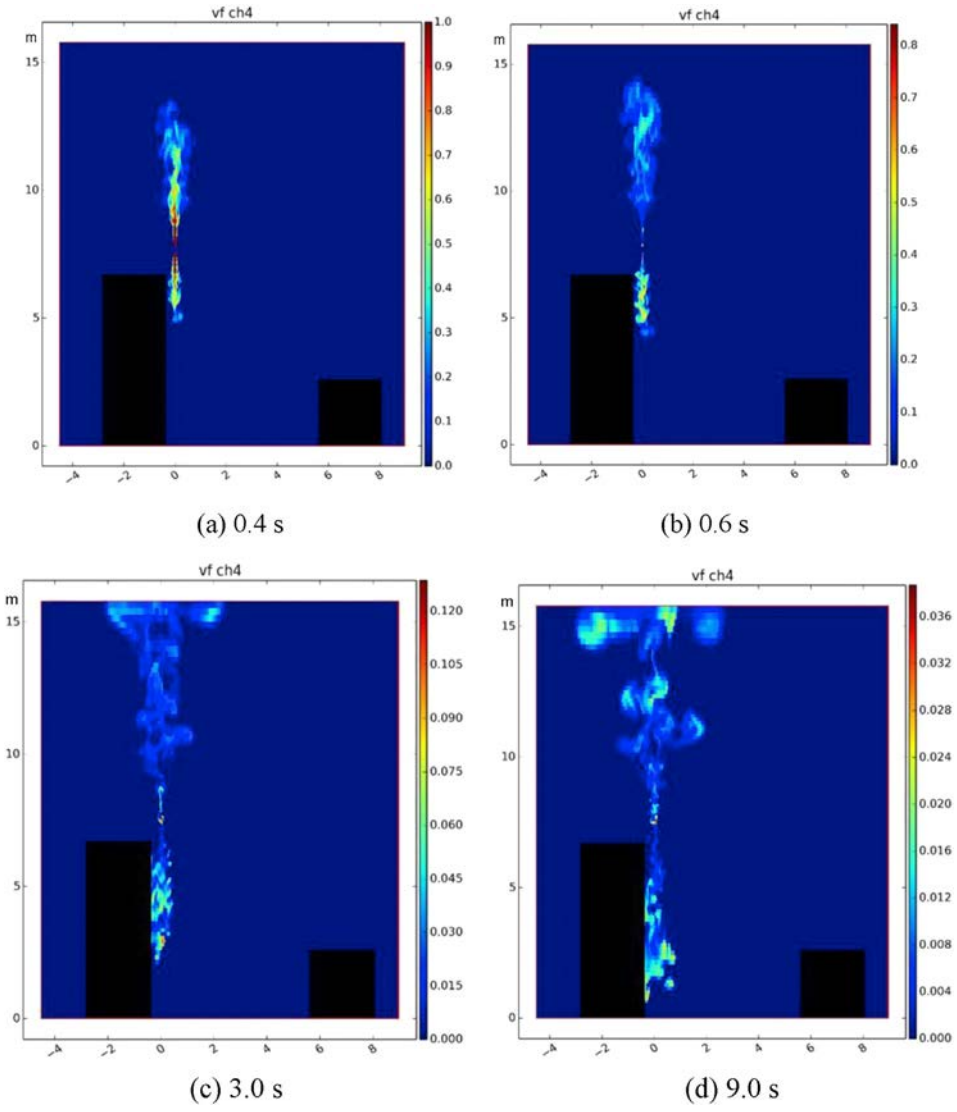

(a) 0.4 s (b) 0.6 s

(c) 3.0 s (d) 9.0 s

Fig. 25 e CH4 volume fraction distribution of version A exhaust tube (x-z view).

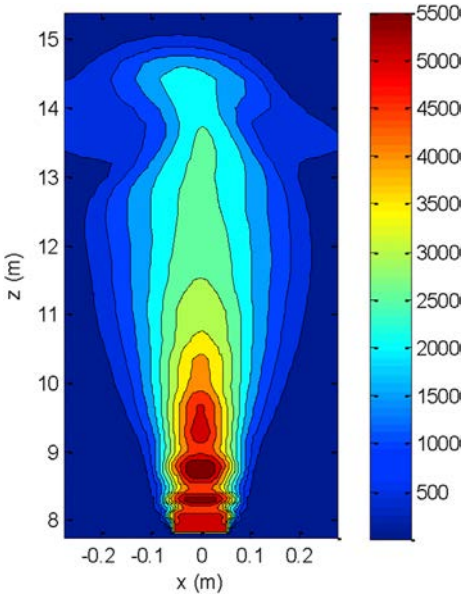

Fig. 26 – Velocity distribution at 0.4s.

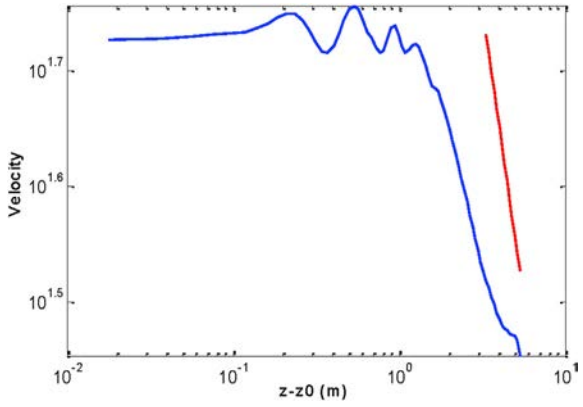

Fig. 27 – Centerline velocity distribution at 0.4s.

3) of carbon monoxide, a lethal exposure concentration of 10 min is 1700 ppm. In case of the sygas/hydrogen with version A exhaust tube, concentrations near ground level exceed this value considerably in the first 20 s, as shown in Fig. 20. For the version B, on the other hand, most of the carbon monoxide is above 5 m and relatively far from ground level, as shown in Figs. 21 and 22.

Because of the immediate danger caused by carbon mon oxide concentrations, version B of the exhaust tube should be chosen over version A in the present case, although the con centrations decrease rapidly within the first minute.

Methane release case

The second scenario is the methane unintended release where we focus on the distribution of the methane cloud and its flammability. The local global two step strategy, including the local model (Model I) and the global model (Model II), is used to model the methane cloud distribution around the methanation plant efficiently and accurately. The

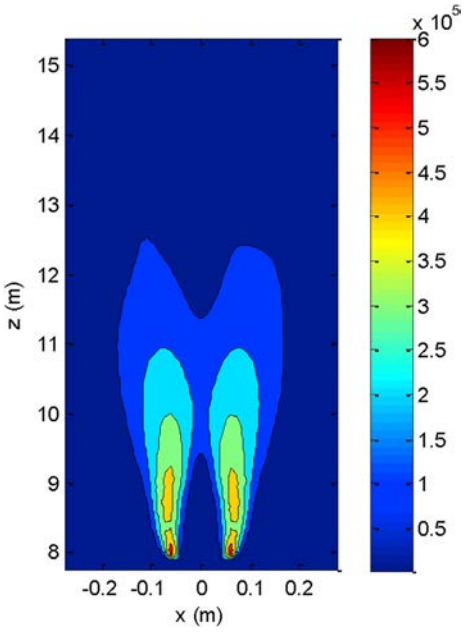

Fig. 28 – Turbulent energy distribution at 0.4s.

performances of two different types of exhaust tubes are calculated and compared.

By using the local model (Model I), the time variant mass fluxes of two different types of the exhaust tubes are calculated, as shown in Figs. 23 and 24. For the top port of version A exhaust tube, the mass flux decreases from 1100 g/s to 900 g/s during the first 0.42s with the increase of gas release in the three phase reactor. Similar to the syn gascase, the mass flux of the top port is about four times larger than that of the bottom port for the version A exhaust tube. There is a significant random fluctuation of mass flow from both ports due to the strong turbulence. For the version B exhaust tube, the area of the top port is much larger than that of the hole at the bottom, therefore, the mass flux from the top port is about seventy times larger than that from the bottom hole. It costs about 0.41 s where the tank pressure gradually decreases from the initial 25 bar to the closing pressure of the safety valve (20 bar). So the time variant mass fluxes during the period between 0 s and 0.41 s are used as the inlet boundary condition for the global flammability evaluation.

The explosion hazard caused by methane gas is assessed by using the global model (Model II). The explo sive range of methane in air is 5.9%–16.0%. The methane distribution of the Version A exhaust tube is presented in Fig. 25. At the early phase of the release, the high speed methane is released from the exhaust tube due to tank overpressure. These two vertical turbulent jets mix with the surrounding air under the free shear force and the numerous turbulence eddy structures could be observed, as shown in Fig. 25(a). This vigorous release process lasts to 0.41 s until the safety valve is closed again. Compared with the methane in the upper space, the methane at ground level should be paid more attention because it is close to the human activity area. Due to the inertia and

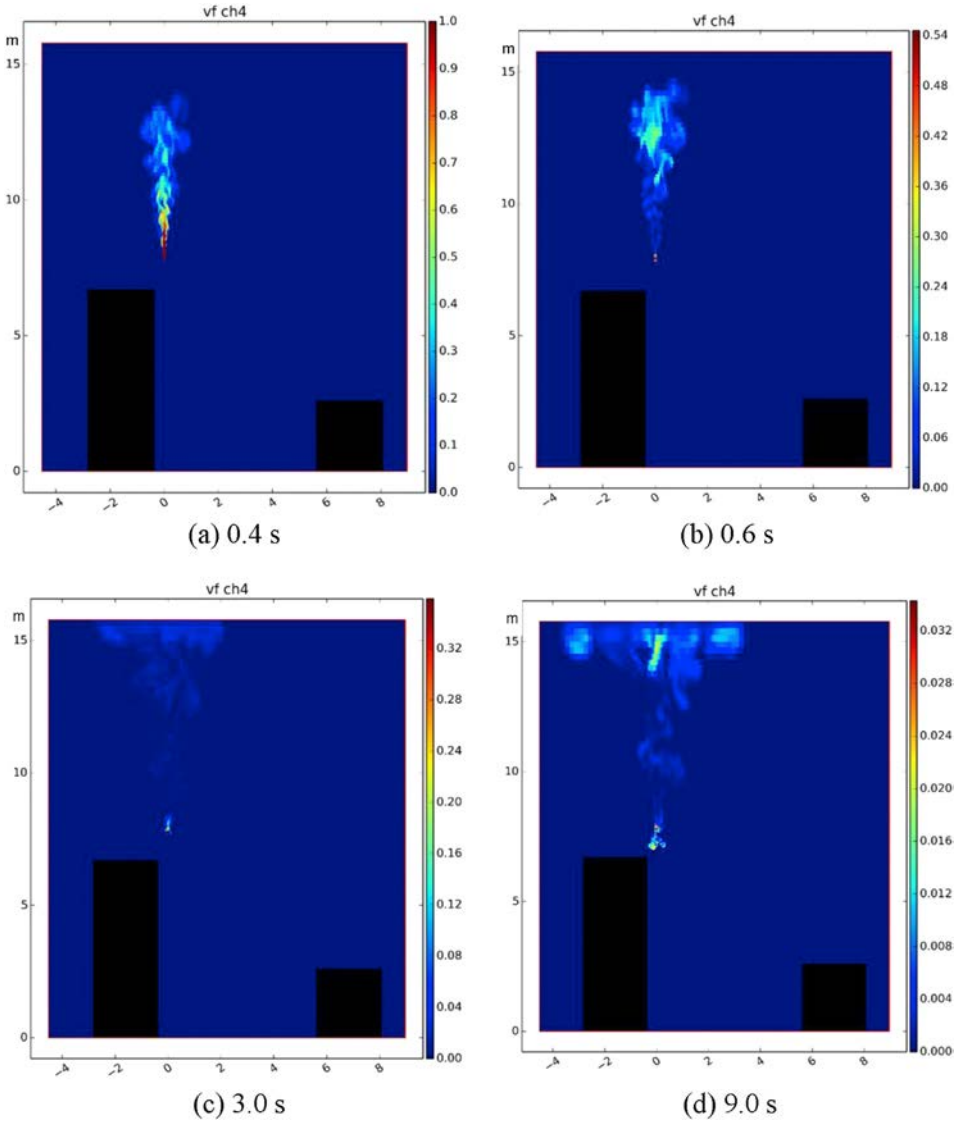

Fig. 29 – CH4 volume fraction distribution of version B exhaust tube (x-z view).

gravity effect, the downward jet further flows toward the ground after the safety valve is closed, as shown in Fig. 25(b–d). The volume fraction of methane is under the lower explosive limit (5.9%) from 9.0s after the release.

The local velocity distribution of the upward jet at 0.4s is presented in Fig. 26, and the centerline velocity is shown in Fig. 27. It could be observed that the velocity near the nozzle is almost kept as a constant which is the potential core region [19]. In this potential core region, it is a steady axisymmetric laminar flow, where the axisymmetric shear layer between the entering fluid and ambient fluid causes a Kelvin–Helmholtz instability [19]. As a consequence, the potential core reaches its end due to the instability devel opment, meanwhile, the flow begins to transform from the laminar state to the turbulent state, and the centerline beginning to decay. Due to the random turbulent fluctua tion, the gas component distribution and velocity distribution are non axisymmetric, as shown in Figs. 25 and 26. In this case, the centerline velocity begins to decay for the region 1 m far away from the nozzle, moreover, the decay slope of the centerline velocity is z^{-1} which is consistent with the theoretical result [21]. The turbulent energy distribution is shown in Fig. 28. The turbulent energy is large in the free shear layer near the nozzle due to the large velocity gradient between the mainstream and the steady state air. This turbulent fluctuation would enhance the mass and momentum transport between the methane and the air in the free shear layer. For the region far away from the nozzle, the velocity gradient becomes small because the free shear force reduces the velocity of the jet flow. Therefore, the turbulent energy in the free shear layer is also deceased.

For the Version B exhaust tube, most methane is released into the upper space from the top port, and just one

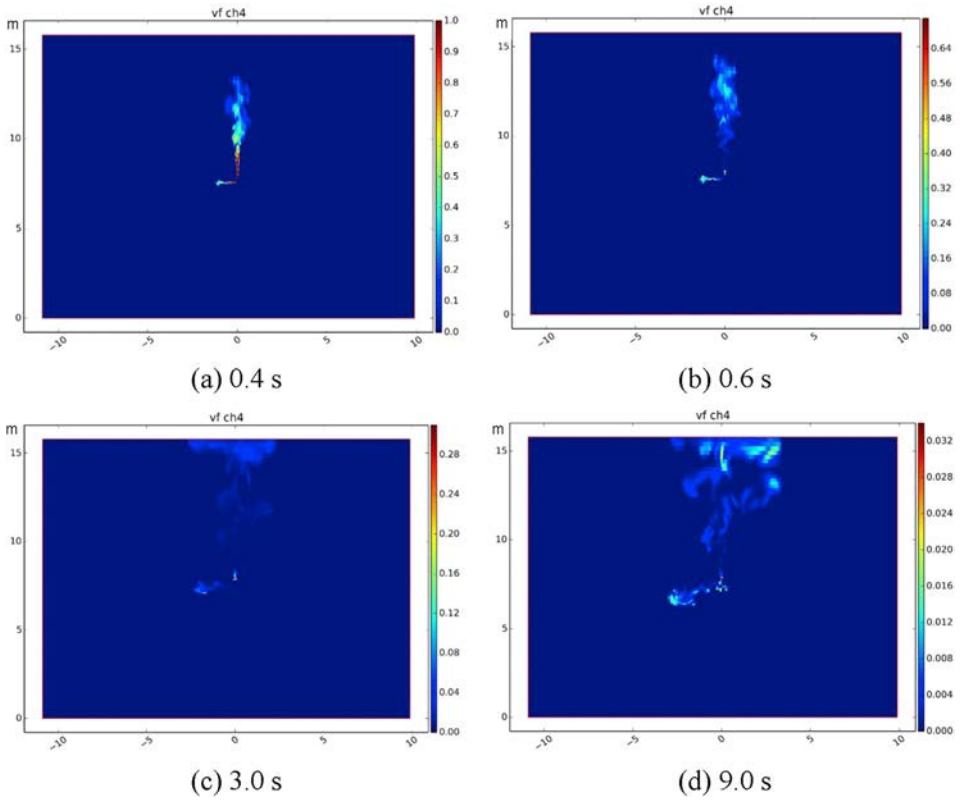

Fig. 30 – CH4 volume fraction distribution of version B exhaust tube (y-z view).

seventieth of the methane is released from the small hole at the height of about 8 m and further diluted by the air, as shown in Figs. 29 and 30. As a result, compared with the Version A exhaust tube, it is much less methane near the ground for the Version B exhaust tube. Moreover, the maximum methane volume fraction of Version B exhaust tube at the 9.0s is also under the lower explosive limit (5.9%).

Conclusions

Since the safety valves of the methanation plant release hazardous gases into the environment in case of over pressure which may threaten the safety of the workers and other humans near the plant, the safety evaluation is per formed in this work using the numerical tool GASFLOW MPI. In detail, two typical accidental scenarios of a prac tical pilot plant built in a modified 40 foot shipping container located at KIT are analyzed and discussed. Due to the all speed capability of GASFLOW MPI, the transient dispersion process could be calculated directly within a local global two step framework without any further assumption model like the notional nozzle model. Several conclusions can be listed as below:

1) For the local model (Model I), the detailed release behaviors of the hazard gases could be resolved directly without any further assumption, including the shock wave structures, time depended pressure in the tank and the transient mass flux through the exhaust tube. For both accidental scenarios, the mass flux of the top port is about four times larger than that of the bottom port in the version A exhaust tube. For version B exhaust tube, the mass flux from the top port is about seventy times larger than that from the bot tom hole, since the area of the bottom hole is much smaller than that of the top port.
2) In the syngas release case, the global dispersion calculation (Model II) show that the hydrogen volume fraction of both the version A and version B exhaust tubes are below the lower explosive limit of hydrogen when it reaches 10 s. While for the toxicity evaluation, the CO concentrations exceed the critical value considerably for both the version A and version B exhaust tubes during the first 20 s but decrease rapidly within the first minute. Moreover, the performance of version B is prior to that of version A from the viewpoints of both the toxicity of carbon monoxide and the flammability of hydrogen because with version B dangerous gas concentrations near ground level can be avoided.
3) In the methane release case, it shows that there are two vertical turbulent jets for version A exhaust tube in the global dispersion model (Model II), and the volume fraction of methane is under the lower explosive limit when it reaches 9.0 s. While for the Version B exhaust tube, most methane is released into the upper space from the top port.

The calculations show, that in the present case, Version B exhaust tube can be considered the safer version and should be chosen over Version A. The analysis of exhaust tube shock interaction will be studied in the future research plan.

Declaration of competing interest

The authors declare that they have no known competing financial interests or personal relationships that could have appeared to influence the work reported in this paper.

REFERENCES

[1] Schiebahn S, Grube T, Robinius M, Tietze V, Kumar B, Stolten D. Power to gas: technological overview, systems analysis and economic assessment for a case study in Germany. Int J Hydrogen Energy 2015;40(12):4285 94.

[2] Iaquaniello G, Setini S, Salladini A, De Falco M. CO2 valorization through direct methanation of flue gas and renewable hydrogen: a technical and economic assessment. Int J Hydrog Energy 2018;43(36):17069 81.

[3] Venetsanos AG, Papanikolaou E, Cariteau B, Adams P, Bengaouer A. Hydrogen permeation from CGH2 vehicles in garages: CFD dispersion calculations and experimental validation. Int J Hydrogen Energy 2010;35(8):3848 56.

[4] Puttock JS. Comparison of thorney island data with predictions of HEGABOX/HEGADAS. J Hazard Mater 1987;16:439 55.

[5] Middha P. Development, use, and validation of the CFD tool FLACS for hydrogen safety studies. PhD thesis. University of Bergen; 2010. https://bora.uib.no/bitstream/1956/4052/1/Dr. thesis Prankul%20Middha.pdf.

[6] Giannissi SG, Venetsanos AG. A comparative CFD assessment study of cryogenic hydrogen and LNG dispersion. Int J Hydrog Energy 2019;44(17):9018 30.

[7] Kudriakov S, Dabbene F, Studer E, Beccantini A, Magnaud JP, Paillère H, Bentaib A, Bleyer A, Malet J, Porcheron E, Caroli C. The TONUS CFD code for hydrogen risk analysis, physical models, numerical schemes and validation matrix. Nucl Eng Des 2008;238:551 65.

[8] Agranat VM, Tchouvelev AV, Cheng Z, Zhubrin SV. CFD modeling of gas release and dispersion: prediction of flammable gas clouds. Adv Combust Aero thermal Technol 2007:179 95.

[9] Wilkening H, Baraldi D. CFD modelling of accidental hydrogen release from pipelines. Int J Hydrogen Energy 2007;32(13):2206 15.

[10] Kashi E, Mirzaei F, Mirzaei F. Analysis of gas dispersion and ventilation within a comprehensive CAD model of an offshore platform via computational fluid dynamics. J Loss Prev Process Ind 2015;36:125 33.

[11] Manogaran S. Modeling of hydrogen and methane dispersion process in pipeline using computational fluid dynamic (CFD). University Malaysia Pahang; 2014. http://umpir.ump.edu.my/id/eprint/9244/1/cd8523.pdf.

[12] Li W, Yu L, Hao J, Li M. Experimental and CFD investigation on flow behaviors of a NPP pump under natural circulation condition. Sci Technol Nucl Installations 2019;2019:5250894. https://doi.org/10.1155/2019/5250894. 10 pages.

[13] Wang M, Wang L, Wang X, Ge J, Tian W, Qiu S, Su G. CFD simulation on the flow characteristics in the PWR lower plenum with different internal structures. Nucl Eng Des 2020;364. 110705.

[14] Ricciardi G. Numerical investigation of fluid forces acting on a confined cylinder with obstacle subjected to axial flow. Sci Technol Nucl Installations 2020;2020:5809175. https://doi.org/10.1155/2020/5809175. 10 pages.

[15] Fiates J, Vianna SV. Numerical modelling of gas dispersion using OpenFOAM. Process Saf. Environ. 2016;104:277 93.

[16] Papanikolaou EA, Venetsanos AG, Heitsch M, Baraldi D, Huser A, Pujol J, Garcia J, Marcatos N. HySafe SBEP V20: numerical studies of release experiments inside a naturally ventilated residential garage. Int J Hydrogen Energy 2010;35(10):4747 57.

[17] Middha P, Hansen OR. CFD simulation study to investigate the risk from hydrogen vehicles in tunnels. Int J Hydrog Energy 2009;34:5875 86.

[18] Gu X, Zhang J, Pan Y, Ni Y, Ma C, Zhou W, Wang Y. Hazard analysis on tunnel hydrogen jet fire based on CFD simulation of temperature field and concentration field. Saf Sci 2020;122:104532.

[19] Zhang H, Li Y, Xiao J, et al. Large eddy simulations of the all speed turbulent jet flow using 3 D CFD code GASFLOW MPI. Nucl Eng Des 2018;328:134 44.

[20] Xiao J, Breitung W, Kuznetsov M, et al. GASFLOW MPI: a new 3 D parallel all speed CFD code for turbulent dispersion and combustion simulations Part I: models, verification and validation. Int J Hydrogen Energy 2017;42:8346 68.

[21] Zhang H, Li Y, Xiao J, et al. Detached Eddy Simulation of hydrogen turbulent dispersion in nuclear containment compartment using GASFLOW MPI. Int J Hydrogen Energy 2018;43:13659 75.

[22] Zhang H, Li Y, Xiao J, Travis JR, Jordan T. Numerical study of the stratification erosion benchmark for NPPs containment using CFD code GASFLOW MPI. Ann Nucl Energy 2019;132:199 211.

[23] Royl P, Xiao J, Jordan T. Blind simulations of Thai test TH27 with GASFLOW MPI for participation in the international benchmark conducted within the German Thai program. In: Workshop application of CFD/CFMD codes september 13 15, cambridge, MA, USA; 2016.

[24] Li Y, Xiao J, Zhang H, et al. Analysis of transient hydrogen release, dispersion and explosion in tunnel with fuel cell vehicles using all speed CFD code GASFLOW MPI. Adelaide, Australia: 8th International Conference on Hydrogen Safety; September 2019. p. 24 6.

[25] Li Y, Zhang H, Xiao J, et al. Numerical study of thermal hydraulics behavior on the integral test facility for Passive Containment Cooling System using GASFLOW MPI. Ann Nucl Energy 2019;123:86 96.

[26] Tong LL, Deng J, Cao XW. Numerical investigation on erosion of hydrogen stratification by steam jet within a local compartment. Int J Energy Res 2020;44:2665 81.

[27] Tong LL, Guo D, Wang D, Cao XW. Improvements of turbulence model for analysis of hydrogen stratification erosion by turbulent buoyant jet. Ann Nucl Energy 2021;150:107797.

[28] Lyu X, Lee X, Ji K, et al. Impact of inert gas injection rate on reducing hydrogen risk during AP1000 post inerting. Ann Nucl Energy 2017;110:230 3.

[29] Lyu X, Xun Z, Ji K, et al. Analysis on hydrogen control system in AP1000 NPP. Ann Nucl Energy 2018;113:279 85.

[30] Lefebvre J, Götz M, Bajohr S, Reimert R, Kolb T. Improvement of three phase methanation reactor performance for steady state and transient operation. Fuel Process Technol 2015;132:83 90.

[31] Technischer Hinweis Merkblatt DVGW G 442 (M). Potentially explosive atmosphere at exhaust opening of venting lines at gas plants or systems. 2015. https://shop.wvgw.de/var/assets/leseprobe/509402 lp%20G%20442.pdf.